The Journal of Neuroscience, January 15, 2001, 21(2):412–422

Calcium Channel Isoforms Underlying Synaptic Transmission at Embryonic *Xenopus* Neuromuscular Junctions

Christopher Thaler, Weiyan Li, and Paul Brehm

Department of Neurobiology and Behavior, State University of New York at Stony Brook, Stony Brook, New York 11794

Studies on the amphibian neuromuscular junction have indicated that N-type calcium channels are the sole mediators of stimulus-evoked neurotransmitter release. We show, via both presynaptic and postsynaptic voltage-clamp measurements, that dihydropyridine (DHP)-sensitive calcium channels also contribute to stimulus-evoked release at developing *Xenopus* neuromuscular junctions. Whereas inhibition of postsynaptic responses by ω-conotoxin (ω-Ctx) GVIA has been taken previously as evidence that only N-type channels mediate transmitter release, we find that both N-type and DHP-sensitive calcium currents are sensitive to this toxin. The unusual sensitivity of DHP-sensitive calcium channels to ω-Ctx GVIA in presynaptic terminals raises the possibility that this channel type may have escaped detection in previous physiological studies on adult frog neuromuscular junctions. Alternatively, the additional channel isoforms may be present only during early development, when they may serve to strengthen collectively presynaptic release during critical periods of synaptogenesis.

Key words: conotoxin; dihydropyridine; acetylcholine receptor; exocytosis; end plate current; spinal neuron

The importance of voltage-dependent calcium channels in neurotransmitter release from presynaptic terminals has long been appreciated (Katz and Miledi, 1967). Several types of voltage-dependent calcium channels, termed L, N, T, P/Q, and R, have been identified (Nowycky et al., 1985; Llinas et al., 1989; Ellinor et al., 1993; Randall and Tsien, 1995). Determining which of these are involved in neurotransmitter release is key to understanding the basic mechanisms of exocytosis and synaptic function. For example, only certain calcium channel isoforms may physically couple to components of the exocytotic machinery (Leveque et al., 1994; Sheng et al., 1994; Butz et al., 1998). In the CNS it appears common that multiple types of calcium channels participate in transmitter release at a single synapse (for review, see Dunlap et al., 1995). By contrast, it is widely held that release at peripheral neuromuscular junctions is mediated by a single type of calcium channel. In frog, it is the N-type channel that is thought to mediate transmitter release (Kerr and Yoshikami, 1984; Robitaille et al., 1990), whereas the P/Q-type channels subserve this function at mammalian neuromuscular junctions (Protti et al., 1996). These findings are somewhat unexpected in view of the immunohistochemical and electrophysiological studies indicating the coexistence of additional calcium channel isoforms in presynaptic terminals of mammalian and amphibian neuromuscular junctions (Day et al., 1997; Yazejian et al., 1997; Westenbroek et al., 1998).

The identification of calcium channel types underlying synaptic transmission has been based primarily on pharmacological profiles provided via inhibition of either postsynaptic responses or directly measured transmitter release (Luebke et al., 1993; Turner et al., 1993; Regehr and Mintz, 1994). Few studies have taken the direct approach of recording both presynaptic calcium current and the associated postsynaptic response, primarily because of the small size and inaccessibility of most synapses. Exceptions include the calyx of Held (Borst et al., 1995), the calyx of the chick ciliary ganglion (Stanley and Goping, 1991; Yawo and Momiyama, 1993), and the giant synapse in squid (Llinas et al., 1981). Recently, Yazejian et al. (1997) introduced the *Xenopus* nerve and muscle coculture system as a preparation in which both the presynaptic and postsynaptic elements are amenable to voltage-clamp recording. Additionally, this synapse has been extensively studied, and *in vitro* development (Anderson et al., 1979; Kidokoro et al., 1980) mirrors many of the morphological and functional properties of those formed *in vivo* (Kullberg et al., 1977). For example, *in vitro* this synapse exhibits precocious postsynaptic development as exemplified by the appearance of junctional folds (Peng et al., 1980) and the localization of acetylcholine receptors (Anderson et al., 1977; Kidokoro and Brass, 1985). In the presynaptic cell, vesicles cluster on the cytoplasmic face of presynaptic densities (Takahashi et al., 1987; Buchanan et al., 1989). The ability to recapitulate such a well defined synapse in culture makes the *Xenopus* nerve and muscle coculture system ideally suited to address questions requiring direct examination of presynaptic and postsynaptic currents such as the identification of calcium channels involved in release.

In this study, we have exploited the advantages of the *Xenopus* preparation to examine directly and dissect pharmacologically presynaptic calcium currents at the neuromuscular junction. Our studies reveal that, unexpectedly, at least two distinct calcium channel types are coupled to release at this synapse.

MATERIALS AND METHODS

Cell culture. To prepare nerve and muscle cocultures, we placed stage 20–22 *Xenopus laevis* embryos (Nieuwkoop and Faber, 1956) in dissecting solution (in mM; 67 NaCl, 1 KCl, 1 $CaCl_2$, and 10 HEPES with 100 U/ml penicillin–streptomycin, taken to a pH of 7.2 with NaOH) and then dissected out the dorsal portion of the animal with tungsten needles. The dorsal portions were then placed in dissecting solution containing 1 mg/ml collagenase (Life Technologies, Gaithersburg, MD) to facilitate separation of the myotomal muscle and spinal cord from any unwanted

Received Aug. 7, 2000; revised Oct. 19, 2000; accepted Oct. 30, 2000.

This research was supported by National Institutes of Health Grant NS-18205. We thank Regeneron for their generous donation of NT-3. Drs. Shcherbatko and Naranjo provided helpful advice during the course of the project. Thanks also to P. Speh for drawing Figure 1.

Correspondence should be addressed to Dr. Paul Brehm at the above address. E-mail: Pbrehm@notes.cc.sunysb.edu.

adherent tissue. Muscle and spinal cords were placed in a Ca^{2+} and Mg^{2+}-free dissecting solution in which they were allowed to dissociate and then were placed on Matrigel (Collaborative Biomedical Products)-coated round glass coverslips (Assistent; Carolina Biological Supply) in a serum-free culture media. After 1 hr they were placed in culture media containing 60% Leibovitz's L-15 medium to which 10 mM Na-HEPES, 100 U/ml penicillin–streptomycin, 20 nM Neurotrophic Factor-3 (Regeneron, Tarrytown, NJ), 1 μM testosterone propionate (Sigma, St. Louis, MO), and 0.5% horse serum were added. The cultures were kept in a dark environment at ~20°C.

Cells in culture were visualized using a Zeiss 63× LD Achroplan objective and identified primarily on the basis of morphology. Spinal neurons appeared as rounded cells with diameters ranging from 10 to 15 μm. Muscle cells could be easily identified by their prominent striations and size, sometimes reaching >200 μm in length. In some cases, when neurites projecting from spinal neurons came into contact with skeletal muscle cells, regional swellings termed varicosities developed that ranged in diameter from 1 to 4 μm. Addition of the Neurotrophic Factor-3 to the culture media increased both the length and number of neurites as well as the size of varicosities. Testosterone also helped to increase the size of varicosities.

Electrophysiology. All voltage-clamp recordings of calcium currents from varicosities were performed via the use of the perforated-patch method (Horn and Marty, 1988). Patch electrodes were made from borosilicate glass (Garner glass type, 7052), and the tips were coated with wax (catalog #72660; Electron Microscopy Sciences, Fort Washington, PA) to decrease the pipette capacitance. The electrode was fire polished to a pipette resistance between 2 and 4 MΩ, and the tip was dipped for 5–10 sec in an internal solution consisting of (in mM) 52 $CsCH_3SO_4$, 38 CsCl, 1 EGTA, 5 HEPES, and 50 glucose, taken to a pH of 7.2 with CsOH. The electrode was then backfilled with internal solution containing 200 μg/ml amphotericin B (Hartsel et al., 1994) and used immediately. The series resistance was monitored after formation of the gigaseal for effects of the amphotericin. Access resistances of 22 MΩ or less were deemed acceptable, and 50% series resistance compensation was used with a 10 μsec lag time. Voltage errors because of liquid junction potentials corresponded to 10 mV on the basis of estimated values (Barry and Lynch, 1991) and direct measurements (Neher, 1992), and all data were corrected for this error.

Recordings from varicosities were complicated by the connections to neurites, resulting in poor voltage control. To reduce the resulting space-clamp artifacts, we used a variation of the method introduced by Katz and Miledi (1967) in which calcium was locally applied to restricted regions of the presynaptic terminal. In our case, the local application of calcium served to restrict activation of calcium current to the varicosity. The nerve and muscle cells were placed in a bath solution consisting of (in mM) 80 tetraethylammonium chloride (TEACl), 10 NaCl, 2 KCl, 5 $MgCl_2$, 5 HEPES, 0.4 $CaCl_2$, 3 glucose, and 1 $MnCl_2$ plus 1 μM tetrodotoxin (Alomone Labs) taken to a pH of 7.2 with *N*-methyl-D-glucamine. This bath solution effectively blocked all voltage-activated conductances. A puffing pipette with an inner diameter of ~4 μm was placed in direct apposition to a sucking micropipette with an inner tip diameter of ~10 μm (Fig. 1). Separate manipulators were used for independent positioning of both the puffing and sucking pipettes. Proper adjustment of positive pressure in the puffing pipette and negative pressure in the sucking pipette allowed the creation of a laminar flow of solution that could be used to apply focally a high-calcium, Mg^{2+} and Mn^{2+}-free solution to presynaptic terminals (Fig. 1). Calcium channels outside of the laminar flow were blocked by the manganese in the bath, whereas those channels in the path of the laminar flow were relieved from block and given access to "high" concentrations of calcium. All drugs including ω-conotoxin (ω-Ctx) GVIA (Alomone Labs), ω-Ctx MVIIC, ω-Agatoxin IVA (Aga IVA) (Peptides International), nitrendipine (Biomol, Plymouth Meeting, PA), Bay K8644 (Sigma), and nimodipine (Research Biochemicals, Natick, MA) were diluted from a stock solution to the working concentration just before use to ensure viability. Dihydropyridines were kept as stock solutions in DMSO. Each drug was delivered via a quartz filament placed within 2 mm of the tip of the puffer pipette. To prevent unwanted mixing of control and drug solutions in the puffer pipette, an air gap separated the individual solutions before injection through the quartz filament. In this way, complete solution exchange in the puffer could be obtained within 2 min. During the entire time course of drug application, the pressure on individual suck and puff electrodes was held constant.

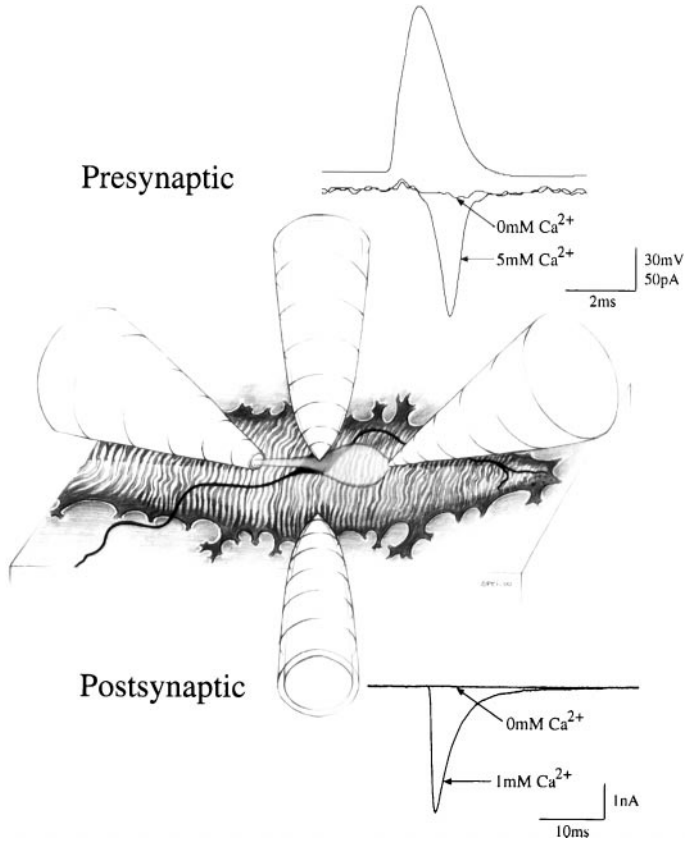

Figure 1. Graphical representation of the electrode configuration used to isolate calcium currents generated by varicosities. Shown are the presynaptic (*top*) and postsynaptic (*bottom*) electrodes as well as the puffer (*right*) and sucker (*left*) pipettes. The puff–suck method was used to deliver a laminar stream of high-calcium solution to limit transmitter release to single varicosities and as a means to apply calcium channel agonists and antagonists focally. *Insets*, Representative *traces* of presynaptic calcium current in response to an action potential command waveform (*top*) and a postsynaptic end plate current (*bottom*) elicited by current injection into a presynaptic terminal are shown. Both presynaptic and postsynaptic current responses are abolished when the puff–suck flow is stopped, exposing both nerve and muscle to the nominally zero calcium-containing solution.

Voltage control over calcium current at each varicosity was optimized by independently adjusting the position and pressure of the puffing and sucking pipettes (Fig. 1). In many varicosities this approach was not successful in providing high-quality voltage-clamp recordings. The quality of the clamp was deemed acceptable only in those recordings in which the inward calcium current (1) began to activate immediately after depolarization, (2) showed graded activation with increasing depolarization, and (3) had associated tail currents that followed an exponential time course.

Voltage-clamp recordings of somatic calcium current were performed using the same materials and methods used for varicosities including the internal, bath, and puffer solutions. In fact the presence of high concentrations of TEA in the bath and puffer used in the present study is the result of our desire to compare somatic and varicosity calcium currents under the same conditions in a future study. The presence of high TEA was necessary to inhibit outward current in somas.

Calcium currents were recorded using EPC-9/2 dual patch-clamp amplifier (Instrutech Corporation) and sampled at 10 μsec intervals. Data were acquired and analyzed using HEKA Pulse+PulseFit software. Before analysis the currents were leak-corrected by use of a P/10 protocol and refiltered with a four-pole Bessel filter at 2 kHz. Current–voltage plots were fit by use of the *I–V* routine in PulseFit (HEKA elektronik) using a combination of the Boltzmann and Goldman–Hodgkin–Katz equations. Calcium currents were evoked by use of either rectangular pulses or action potential waveforms as command pulses. The action

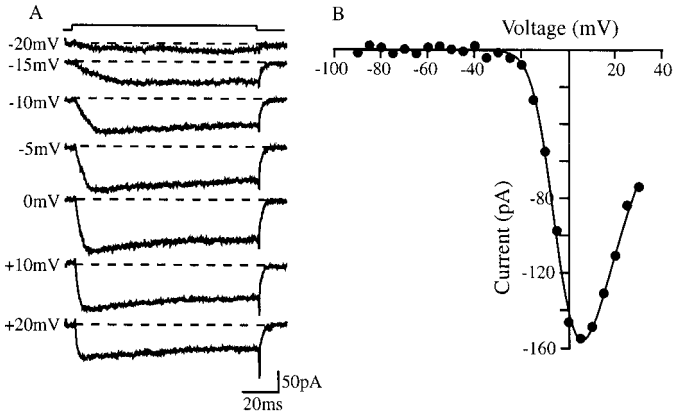

Figure 2. Perforated-patch voltage-clamp recording of calcium currents from a varicosity. *A*, Representative leak-subtracted sweeps recorded in 5 mM calcium elicited by depolarizing steps to the indicated potentials from a holding potential of −90 mV. The *dotted lines* indicate the zero current level. *B*, Current–voltage relations for peak calcium currents from the varicosity represented in *A*. The access resistance was 19 MΩ, and the series resistance compensation was set at 50%.

potential waveform was generated by first recording from varicosities in the current-clamp mode. For this purpose the perforated-patch electrode was filled with an internal physiological solution (IPS) consisting of (in mM) 88 KCH_3SO_4, 10 $NaCH_3SO_4$, 5 HEPES, 2 KCl, and 1 EGTA taken to a pH of 7.2 with KOH. The normal bath solution (NBS) contained (in mM) 110 NaCl, 2 KCl, 2 $CaCl_2$, 1 $MgCl_2$, and 5 HEPES taken to a pH of 7.2 with NaOH. The internal solution lacked Cs^+ and the external solution lacked TEA so that the natural waveform of the action potential could be faithfully recorded. The cell body was stimulated with an extracellular electrode, and the propagating action potential was recorded from the associated varicosity. This action potential was digitized and translated into a command pulse.

In muscle, both spontaneous and evoked synaptic currents were recorded using ruptured whole-cell voltage-clamp techniques. The muscle internal solution consisted of (in mM) 95 KCl, 10 NaCl, 5 HEPES, and 10 EGTA taken to a pH of 7.2 with KOH. The muscle external solution was calcium-free NBS. Synaptic currents were evoked by either of two stimulating methods. In most cases the varicosity was directly depolarized by means of a perforated-patch electrode containing IPS. Alternatively, in some cells the soma, rather than the varicosity, was depolarized, and the endplate current (EPC) was triggered by a propagating action potential.

RESULTS

After 1 d in culture, dissociated *Xenopus* spinal neurons project neurites over distances of hundreds of micrometers. At points of contact with muscle, the neurites occasionally form swellings, termed varicosities, that reach diameters of up to 4 μm. Two lines of evidence indicate that these varicosities represent sites of functional neuromuscular contacts. First, extracellular recordings demonstrated that the majority of spontaneous miniature EPCs (mEPCs) were generated near a varicosity, thus indicating localized release of neurotransmitter (data not shown). In addition, simultaneous presynaptic current-clamp and postsynaptic voltage-clamp recordings showed that varicosities support evoked release (Fig. 1). The release occurs specifically from varicosities as shown by the dependence of EPCs on the presence of local calcium. Both presynaptic calcium current and the associated postsynaptic EPC were abolished when the flow of calcium was stopped by lifting the puffing electrode (Fig. 1).

Voltage-dependent calcium current recorded from presynaptic varicosities ranged in size from undetectable levels to 600 pA when 5 mM calcium was used as the charge carrier. The average threshold for activation of calcium current was −16 ± 6 mV, and on average, the peak current occurred at +10 ± 6 mV (Fig. 2). The inward current trajectory showed a slight decay during a 100-msec-long depolarization (Fig. 2). This decay was not caused by contamination by low-voltage-activated (LVA), fast-inactivating calcium currents. Typically, LVA calcium currents recorded from the cell bodies of spinal neurons activated at −60 mV and completely inactivated at a holding potential of −50 mV (data not shown). In the 49 spinal neuron varicosities recorded in this study, no LVA current was observed. Analysis of inactivation of high-voltage-activated (HVA) current was not performed because long-duration pulses resulted in a rapid loss of calcium current even with the use of perforated-patch techniques. Such loss of calcium current is frequently associated with elevations in intracellular calcium levels that likely accompany prolonged depolarizations (Kostyuk and Krishtal, 1977; Byerly and Hagiwara, 1982). Therefore, we reduced the pulse duration to 10 or 20 msec to minimize calcium charge entry, and this approach dramatically slowed or, in most cases, completely abolished current rundown.

Pharmacological dissection of calcium currents

Various pharmacological blockers of specific calcium channel isoforms were tested for inhibition of peak calcium current. First, the presence of dihydropyridine (DHP)-sensitive calcium current was detected by separate application of the antagonists nitrendipine and nimodipine. Both antagonists were tested at 1 μM for inhibition of varicosity calcium current. Time course measurements indicate that this concentration of DHP antagonist reversibly inhibits calcium current (Fig. 3*A*). Of the nine terminals tested, nitrendipine reduced the calcium current by 28 ± 16% (mean ± SD), with one terminal showing no inhibition of calcium current (see Fig. 7). By comparison, nimodipine inhibited 17 ± 17% of the inward current in the seven cells tested, with three terminals showing no inhibition (see Fig. 7). However, in the 12 cells affected, nitrendipine and nimodipine showed no significant difference in levels of inhibition that averaged 31 ± 12% for nitrendipine and 29 ± 8% for nimodipine (Student's *t* test, $p > 0.05$). Only one of the varicosities exhibited a shift in the current–voltage relations after block by nitrendipine or nimodipine (Fig. 3*B*). However, because the voltage was incremented in 10 mV steps, similar effects of DHP antagonists on the current–voltage relations in other varicosities may have gone undetected. In control experiments application of 0.05% DMSO resulted in no inhibition of varicosity calcium current. The DHP agonist Bay K8644 was also tested for effects on calcium current. In six varicosities examined, 5 μM Bay K8644 had no discernable effect on the peak amplitude of calcium current or decay kinetics of calcium tail current (see Fig. 7), consistent with previously published results (Hulsizer et al., 1991; Meriney et al., 1991).

To determine whether nitrendipine-sensitive calcium channels can contribute to the calcium current under more physiological conditions, action potential waveforms were used. For this purpose, action potentials were recorded from varicosities under current-clamp conditions with potassium rather than cesium in the pipette (see Materials and Methods). The resting potential was −74 ± 3 mV ($n = 10$), and the average action potential peaked at +43 ± 6 mV ($n = 10$) with a half-amplitude duration of 1.4 ± 0.2 msec ($n = 10$). No significant undershoot was detected. In contrast to rectangular pulses, the calcium currents in response to action potential waveforms occurred in coincidence with repolarization (Fig. 3*C*). In three terminals tested, inhibition by nitrendipine was similar (Student's *t* test, $p > 0.05$) for the

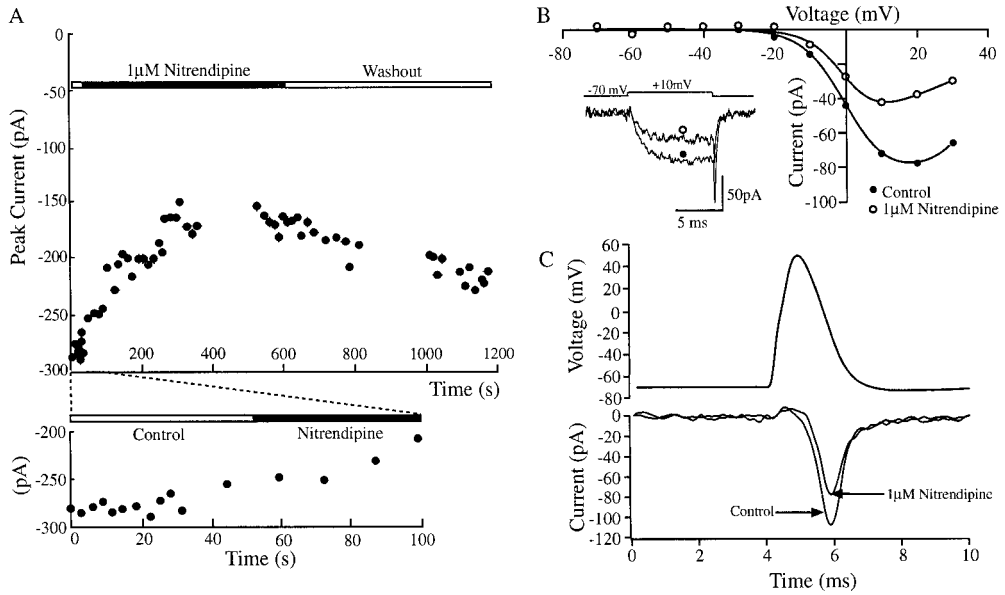

Figure 3. The effect of 1 μM nitrendipine on the calcium current from varicosities. *A*, Time course of inhibition of varicosity calcium current. After a stable baseline was established (*bottom*), application of 1 μM nitrendipine for 4 min resulted in a 48% reduction in the peak calcium current. After exposure to drug-free solution, a partial recovery (to 75% of control) of peak current (*top*) was achieved. *B*, Current–voltage relations of peak calcium current from a different varicosity before (*solid circles*) and 8 min after (*open circles*) continued application of 1 μM nitrendipine. Nitrendipine inhibited the peak HVA current by 47%. *Inset*, Two representative current *traces* elicited by step depolarizations from −70 to +10 mV before (*solid circle*) and after (*open circle*) application of nitrendipine. The access resistance was 22 MΩ, and the series resistance compensation was set at 50%. *C*, Calcium current (*bottom traces*) elicited from the same varicosity shown in *B* using an action potential waveform as the command potential (*top trace*), before and after exposure to 1 μM nitrendipine. Nitrendipine inhibited 35% of the calcium current. Each *trace* is an average of five sweeps.

action potential command waveform (39%) and the rectangular pulse waveform (36%).

Over 60% of the calcium current was therefore generated by DHP-insensitive channels. Further pharmacology was performed to identify the calcium channel isoforms underlying the remaining current. P/Q-type channels have been shown to underlie release at mammalian neuromuscular junctions (Protti et al., 1996). The contribution of P/Q-type channels to the calcium current at *Xenopus* varicosities was tested by applying either 500 nM ($n = 4$) or 1 μM ($n = 1$) ω-Aga IVA to varicosities, concentrations shown to block fully both P- and Q-type channels in cerebellar granule cells (Randall and Tsien, 1995). No significant inhibition of the calcium current was observed in any of the five varicosities tested even after 7 min of exposure to the toxin (Fig. 4; also see Fig. 7).

The potential contribution of N-type channels to HVA calcium current was next investigated. Initially, ω-Ctx GVIA, an N-type calcium channel blocker, was tested for effects on calcium current using both rectangular pulses and action potential command waveforms. Application of 1 μM ω-Ctx GVIA reduced calcium current rapidly such that a saturating block was achieved within 200 sec (Fig. 5*A*). Furthermore, washout of ω-Ctx GVIA resulted in no recovery of inhibited current over a 10 min period. At maximal block, ω-Ctx GVIA reduced the peak current by 91 ± 11% ($n = 10$) for rectangular command pulses (see Figs. 5*B*, 7) and 91 ± 15% for action potential waveforms (Fig. 5*C*; $n = 3$).

The amount of inhibition by ω-Ctx GVIA in response to both action potential waveforms and rectangular pulses was unexpectedly high considering the estimated contribution of DHP-sensitive channel types in varicosities (see Fig. 7). The supra-additive block by ω-Ctx GVIA and DHP antagonists suggests an apparent lack of specificity on the part of either ω-Ctx GVIA or the DHP antagonists nitrendipine and nimodipine. To explore directly the possibility that the DHP antagonists were inhibiting N-type calcium current, we recorded from the cell bodies of spinal neurons. The somas exhibit a large component of ω-Ctx MVIIC-sensitive (Fig. 6*B*) and ω-Ctx GVIA-sensitive (data not shown) calcium current, which forms a basis for testing possible

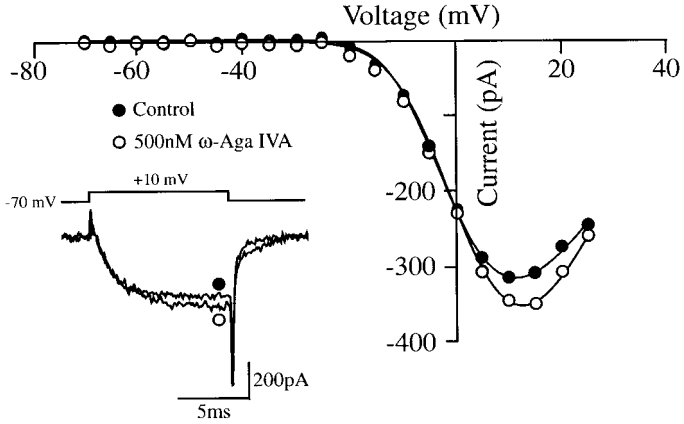

Figure 4. Varicosity calcium currents are insensitive to ω-Aga IVA. Current–voltage relations of peak calcium current before (*solid circles*) and after (*open circles*) application of 500 nM ω-Aga IVA. *Inset*, Two representative calcium current *traces* elicited by step depolarizations from −70 to +10 mV before (*solid circle*) and 5 min after (*open circle*) application of ω-Aga IVA. The access resistance was 19 MΩ, and the series resistance compensation was set at 50%. The increase in inward current with ω-Aga IVA was not consistently observed and is not considered to be toxin mediated.

inhibitory actions of DHP antagonists on N-type calcium current. In 15 somatic recordings, application of 1 μM nitrendipine had no inhibitory effect (data not shown). These findings indicate that DHP antagonists were not inhibiting N-type channels.

To test the alternative possibility that ω-Ctx GVIA inhibits non-N-type channels, we turned to the use of ω-Ctx MVIIC, another N-type blocker. At a concentration of 10 μM, ω-Ctx MVIIC blocks both P/Q- and N-type calcium current (Hillyard et al., 1992; McDonough et al., 1996). Previous experiments on varicosity calcium currents using ω-Aga IVA (Figs. 4, 7) indicated that P/Q-type channels are lacking in varicosities; therefore, any effects of ω-Ctx MVIIC are likely to result from inhibition of N-type current. As done for previous pharmacological inhibitors, ω-Ctx MVIIC was applied to varicosities to establish the time

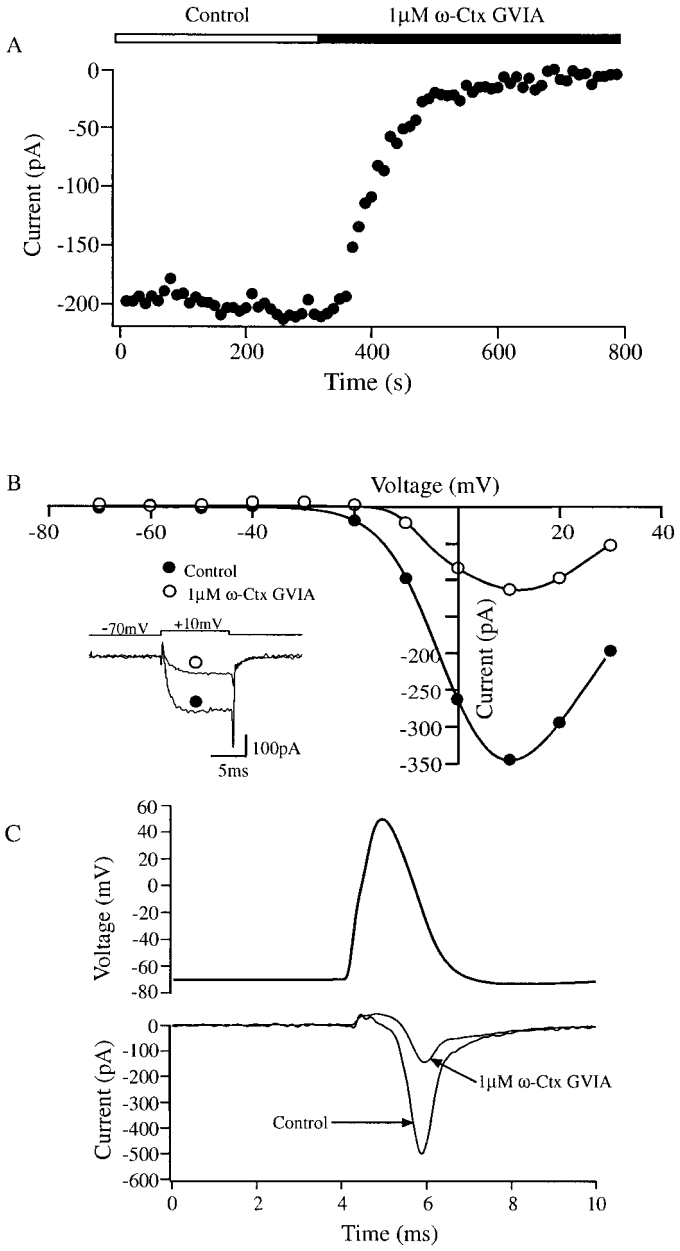

Figure 5. The inhibitory effect of 1 μM ω-Ctx GVIA on calcium current recorded from varicosities. *A*, Time course of inhibition of varicosity calcium current. Application of 1 μM ω-Ctx GVIA for 2 min resulted in an inhibition of 100% of peak calcium current. *B*, Current–voltage relations of peak calcium current from a different varicosity measured before (*solid circles*) and 3 min after (*open circles*) application of 1 μM ω-Ctx GVIA with 5 mM calcium as the charge carrier. The calcium current recorded at +10 mV was inhibited by 68% after exposure to ω-Ctx GVIA. *Inset*, Two representative current *traces* elicited by step depolarizations from −70 to +10 mV before (*solid circle*) and after (*open circle*) application of ω-Ctx GVIA. The access resistance was 22 MΩ, and the series resistance compensation was set at 50%. *C*, Calcium currents from the same varicosity shown in *B* elicited in response to an action potential waveform before and after exposure to 1 μM ω-Ctx GVIA. Seventy-three percent of the peak control current was blocked. Each *trace* is an average of five sweeps. The early outward current associated with the depolarizing phase of the action potential waveform was the result of incorrect leak subtraction often associated with the upstroke of the action potential waveform.

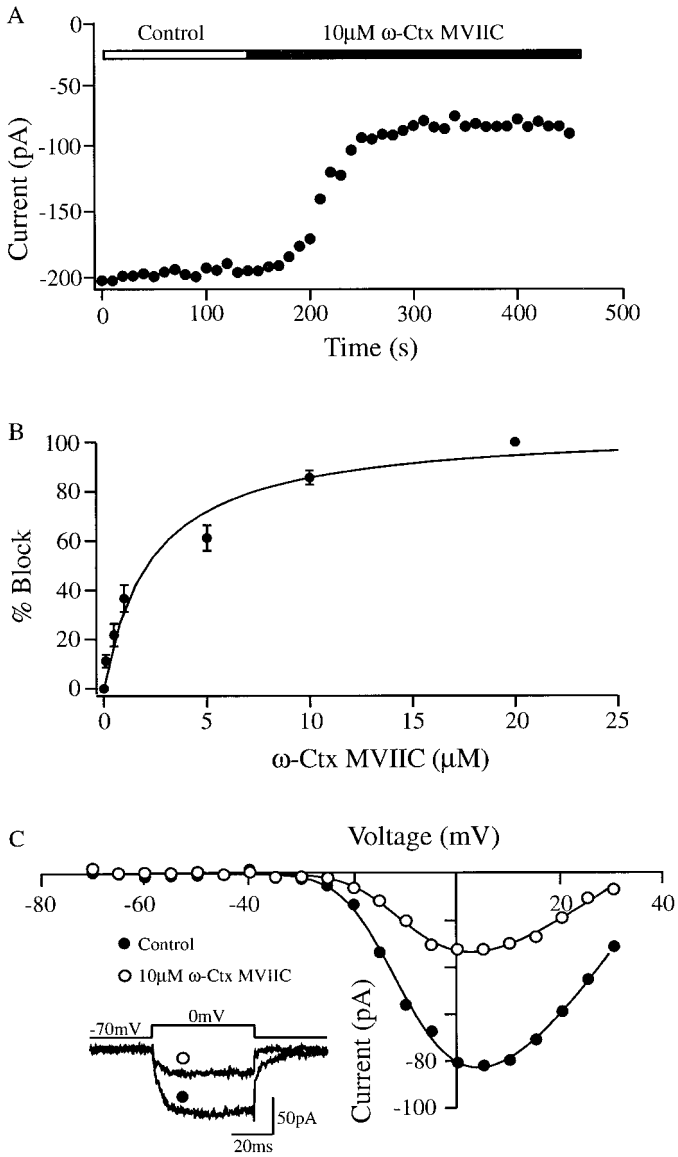

Figure 6. Inhibition of calcium current by ω-Ctx MVIIC. *A*, Time course of inhibition of varicosity calcium current by 10 μM ω-Ctx MVIIC. Exposure to 10 μM ω-Ctx MVIIC for 2 min resulted in an inhibition of 54% of peak calcium current. *B*, Dose–response curve for normalized ω-Ctx MVIIC-sensitive calcium currents recorded from six spinal neuron somas. SEMs are shown for the six cells. Data were fitted with a variation of the Hill equation: $r = R_{max}/(1 + (K/x))$, where $K = IC_{50}$, R_{max} = the maximal percentage of block, r = the percentage of block, and x = toxin concentration. *C*, Current–voltage relations of peak calcium current measured before (*solid circles*) and 7 min after (*open circles*) application of 10 μM ω-Ctx MVIIC with 5 mM calcium as the charge carrier. The calcium current recorded at 0 mV was inhibited by 59% after exposure to ω-Ctx MVIIC. *Inset*, Two representative current *traces* elicited by step depolarizations from −70 to 0 mV before (*solid circle*) and after (*open circle*) application of ω-Ctx MVIIC. The series resistance compensation was set at 50%.

course of calcium current inhibition. ω-Ctx MVIIC time course measurements indicated that equilibrium block was achieved within 2 min at a concentration of 10 μM (Fig. 6*A*). In contrast to ω-Ctx GVIA, application of 10 μM ω-Ctx MVIIC blocked an average of 48 ± 7% (n = 8) of varicosity calcium current (Figs. 6*C*, 7). If a saturating block by ω-Ctx MVIIC is assumed, these lower values also indicate that ω-Ctx GVIA may not provide a block that is N-type specific. To test whether ω-Ctx MVIIC was saturating, we recorded from spinal neuron somas that do not

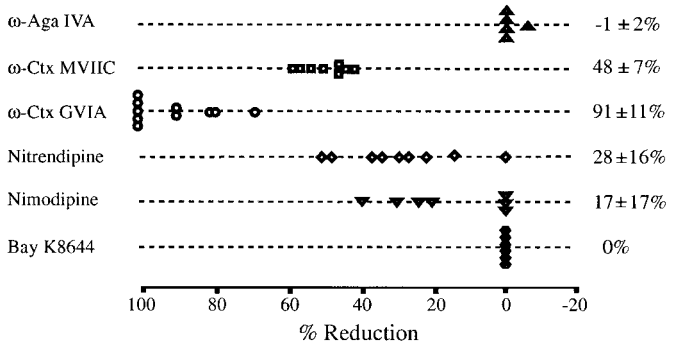

Figure 7. Results of pharmacological inhibition of calcium current. Each *symbol* represents the percent reduction in peak calcium current for individual varicosities. The means and SDs are indicated.

express P/Q-type calcium channels (data not shown) and in which long-term recordings of calcium current could be performed relatively easily. The dose dependence of inhibition indicated that 80% of the ω-Ctx MVIIC-sensitive current was blocked at the 10 μM concentration (Fig. 6*B*). Correcting for the subsaturating block by 10 μM ω-Ctx MVIIC resulted in an overall average inhibition of 60 ± 9% that is significantly less than the 91 ± 11% value obtained for ω-Ctx GVIA (Student's *t* test, $p < 0.05$).

More direct tests of nonspecific block by ω-Ctx GVIA were provided by experiments in which combinations of DHP antagonists, ω-Ctx GVIA, and ω-Ctx MVIIC were sequentially applied in different orders. In the first experiment, 10 μM ω-Ctx MVIIC was applied to a varicosity for 2 min, resulting in a stable inhibition of 43% of peak calcium current. Subsequent application of a solution containing 10 μM ω-Ctx MVIIC and 1 μM nimodipine resulted in a further 25% inhibition, indicating that ω-Ctx MVIIC was not substantially inhibiting DHP-sensitive current (data not shown). Such was not the case when ω-Ctx GVIA was tested after ω-Ctx MVIIC plus nitrendipine. In the experiment shown in Figure 8*A*, 10 μM ω-Ctx MVIIC was applied for 10 min, resulting in a stable 45% block of calcium current. Subsequent application of a solution containing both 10 μM ω-Ctx MVIIC and 1 μM nitrendipine resulted in a further 30% inhibition of current (Fig. 8*A,B*). The combined actions of ω-Ctx MVIIC and nitrendipine inhibited 75% of calcium current. In this same varicosity, block by ω-Ctx MVIIC and nitrendipine was partially reversed by application of drug-free solution. Subsequent exposure of 1 μM ω-Ctx GVIA rapidly and irreversibly blocked 100% of the available calcium current (Fig. 8*A,C*) consistent with a nonspecific blocking effect of ω-Ctx GVIA. In a third example of a multidrug application experiment, 10 μM ω-Ctx MVIIC and 1 μM ω-Ctx GVIA were tested sequentially for their ability to inhibit varicosity calcium current (Fig. 9). ω-Ctx MVIIC (10 μM) resulted in a 40% inhibition of calcium current. Addition of 1 μM ω-Ctx GVIA in the continued presence of 10 μM ω-Ctx MVIIC blocked a further 40% of calcium current. Even after correcting for the subsaturating concentration of ω-Ctx MVIIC, these data indicate that ω-Ctx GVIA is blocking a component of calcium current shown to be ω-Ctx MVIIC insensitive. Importantly, in ~50% of the cells tested ($n = 10$), ω-Ctx GVIA did not provide complete block of calcium current, indicating that there exists a third isoform that is toxin insensitive.

Evoked synaptic current

To assess the contribution of individual calcium channel isoforms to transmitter release, simultaneous recordings of nerve and muscle were made during the application of calcium channel blockers. Spontaneously twitching muscle cells were selected to ensure the presence of a functional contact between the varicosity and the muscle. The presynaptic neuron was current clamped while the associated muscle was simultaneously voltage clamped, thereby inhibiting muscle contraction. An EPC was evoked by depolarization of either the varicosity or the soma to threshold for a presynaptic action potential. The local application of calcium using the puff–suck method ensured that the release of transmitter was occurring from the varicosity and not from distant release sites (Fig. 1). To achieve good voltage control, the muscle was held at −40 mV to decrease the size of the synaptic currents. To verify that the muscle cells were well voltage clamped, the reversal potential of both spontaneous and evoked synaptic currents was measured. Reversal of synaptic currents occurred near 0 mV that is close to the reversal potential for single-channel acetylcholine (ACh)-activated currents (Brehm et al., 1984a).

A potential role of DHP-sensitive calcium channel isoforms in coupling to transmitter release was tested by direct depolarization of the varicosity under current clamp. Nitrendipine was applied to the varicosity for at least 4 min, which was the time required to achieve maximal block of synaptic current. To estimate the inhibition by nitrendipine, 10 EPCs were averaged before and after treatment (Fig. 10*A*). The level of inhibition produced by nitrendipine and other calcium channel antagonists was quantified by a reduction in both peak amplitude and charge entry of the averaged EPCs before and after drug application. In three cells tested, application of nitrendipine caused a peak current reduction of 10 ± 8% and a charge entry reduction of 13 ± 9% (Fig. 10*A*). The method of direct depolarization of the terminal (Fig. 10*A*) resulted in a slight prolongation of the action potential, because of the injection of charge required for the depolarization. To ensure that direct depolarization of the terminal did not alter the contribution by DHP-sensitive channels, we performed additional recordings in which the action potentials were elicited in the cell body (Fig. 10*B*). In three cells tested in this manner, one cell showed no change in EPC amplitude after application of 1 μM nitrendipine. However, in the other cells the EPC amplitude was reversibly decreased by 17 and 15%, resulting in an overall average decrease of 11% (Fig. 10*B*; $n = 3$). This value is not significantly different from that obtained using direct depolarization of the varicosity (Student's *t* test, $p > 0.05$).

The contribution of nitrendipine-insensitive calcium channels to synaptic transmission was determined by measuring effects of conotoxins on postsynaptic responses. ω-Ctx MVIIC (10 μM) was applied to a varicosity for at least 2 min, a period sufficient to achieve maximal block. This resulted in a 57% inhibition in peak current in the cell shown in Figure 11 and a 63% decrease in a second cell. Subsequent addition of 5 μM nitrendipine to this varicosity caused a further 17% reduction, sparing 26% of the synaptic current (Fig. 11). These findings confirm our previous conclusion that ω-Ctx MVIIC does not block nitrendipine-sensitive calcium currents. In this same recording (Fig. 11), a drug-free washout period of 10 min recovered the current to 90%. Addition of 1 μM ω-Ctx GVIA reduced the synaptic current to 11% of the control value, demonstrating that the synaptic current generated by DHP-sensitive channels is targeted by this toxin. The incomplete block by ω-Ctx GVIA supports the idea that the insensitive calcium current can also mediate release. Overall, 1 μM ω-Ctx GVIA resulted in an average 89 ± 8% ($n = 4$) inhibition of peak EPC and a 93 ± 10% ($n = 4$) decrease in EPC-associated charge entry.

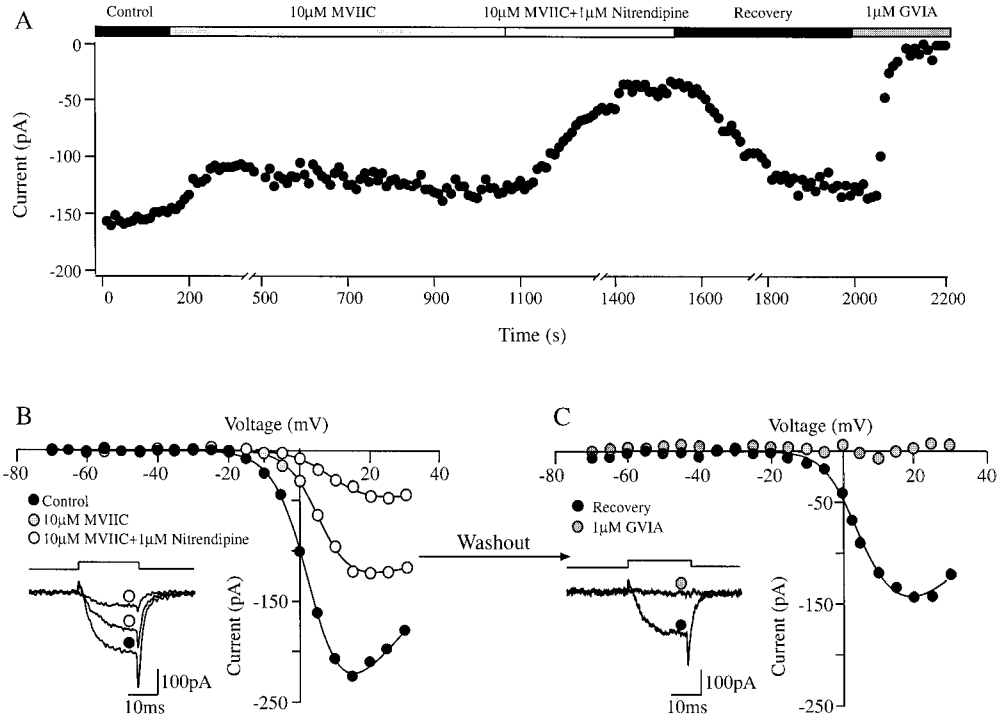

Figure 8. L-type calcium channels are targeted by ω-Ctx GVIA but spared by ω-Ctx MVIIC. *A*, The time course of peak calcium current amplitude in response to sequential drug treatment is indicated. Each *circle* represents a single measurement from the same cell shown in *B* and *C*. Current amplitudes in *A* are slightly different from peak amplitudes in *B* and *C* because a test potential lower than peak voltage was used for the time course measurement. *B*, Current–voltage relations are shown of peak calcium current before exposure to calcium channel antagonists (*solid circles*) and after a 10 min exposure to 10 μM ω-Ctx MVIIC (*gray circles*), followed by a 3 min exposure to 1 μM nitrendipine (*open circles*) in the continued presence of 10 μM ω-Ctx MVIIC. The peak calcium current was inhibited by 45% after 10 μM ω-Ctx MVIIC and by an additional 30% after exposure to 1 μM nitrendipine. *Inset*, Three corresponding, representative current *traces* are shown in response to step depolarizations from a holding potential of −70 mV to the voltage at which maximal current was observed. *C*, After a 10 min drug-free washout, the current recovered to 62% of the control current amplitude (*solid circles*). Application of 1 μM ω-Ctx GVIA irreversibly inhibited the remaining calcium current (*gray circles*). The greater inhibition by ω-Ctx GVIA than by the combined actions of ω-Ctx MVIIC and nitrendipine is likely a result of a subsaturating dose of ω-Ctx MVIIC used. *Inset*, Two representative current *traces* before (*solid circle*) and after (*gray circle*) 1 μM ω-Ctx GVIA are shown. The access resistance was 21 MΩ, and the series resistance compensation was set at 50%.

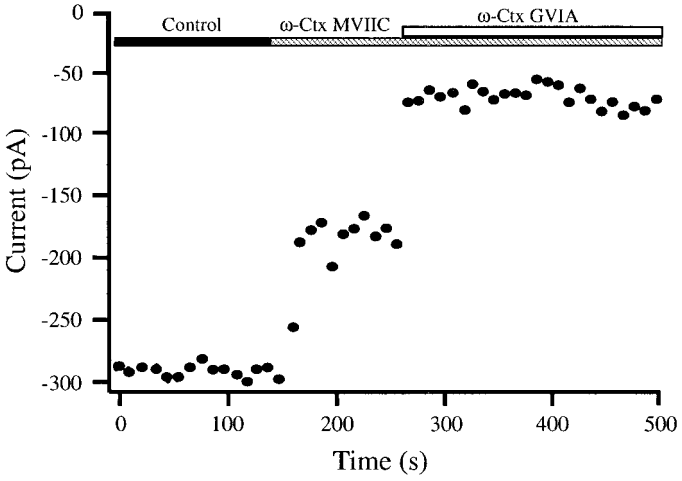

Figure 9. The inhibition of terminal calcium current by consecutive treatments with ω-Ctx MVIIC and ω-Ctx GVIA. Each *point* represents the peak current generated by 10 msec square test pulses to 0 mV from a holding potential of −70 mV. Application of 10 μM ω-Ctx MVIIC inhibited the peak calcium current by 40%. Addition of 1 μM ω-Ctx GVIA in the continued presence of ω-Ctx MVIIC reduced the peak current by an additional 40%. The access resistance was 19 MΩ, and the series resistance compensation was set at 50%.

In all recordings of EPCs the decay of inward current followed an exponential time course. Measurements of EPC decay indicated that exposure to calcium channel antagonists led to a significant acceleration of current decay. For example the average time constant of decay in the control current in Figure 11 was 6.2 ± 1.7 msec before ω-Ctx MVIIC and 3.4 ± 0.4 msec after ω-Ctx MVIIC. This is not a specific consequence of the application of calcium channel inhibitors because a similar relationship between decay rate and EPC amplitude exists in the absence of pharmacological blockers of calcium current. In fact, this relationship between EPC decay rate and amplitude is not likely to involve presynaptic calcium channels. Instead, the slow decay for larger-amplitude EPCs likely reflects the increased time required for clearance of ACh in the synaptic cleft (Del Castillo and Katz, 1956). Evidence of this idea comes from comparisons of evoked and spontaneous currents recorded from the same muscle in which similar relationships between amplitude and decay rates were observed (data not shown).

DISCUSSION

Studies on frog neuromuscular junction have led to the idea that N-type calcium channels play a central role in the release of transmitter. The major impetus for this idea came from studies showing that ω-Ctx GVIA, an antagonist of the N-type calcium channel, abolishes evoked postsynaptic responses (Kerr and Yoshikami, 1984; Koyano et al., 1987; Sano et al., 1987; Katz et al., 1995; Yazejian et al., 1997). Complementary immunocytochemical (Tarelli et al., 1991) and ω-Ctx GVIA-labeling studies (Robitaille et al., 1990) revealed the presence of N-type calcium channels in the active release zones, furthering the evidence that this channel type is responsible for release of ACh. Few studies have tested whether additional calcium channel isoforms, such as the L-type channel, contribute to presynaptic calcium current. The finding that neither L-type agonists nor antagonists altered the photometrically determined calcium current (Robitaille et al., 1996) lends support to the idea that the L-type channels are absent in the terminals. Voltage-clamp measurements of calcium current in developing *Xenopus* nerve terminals indicated that L-type channels are present. However, it was not established

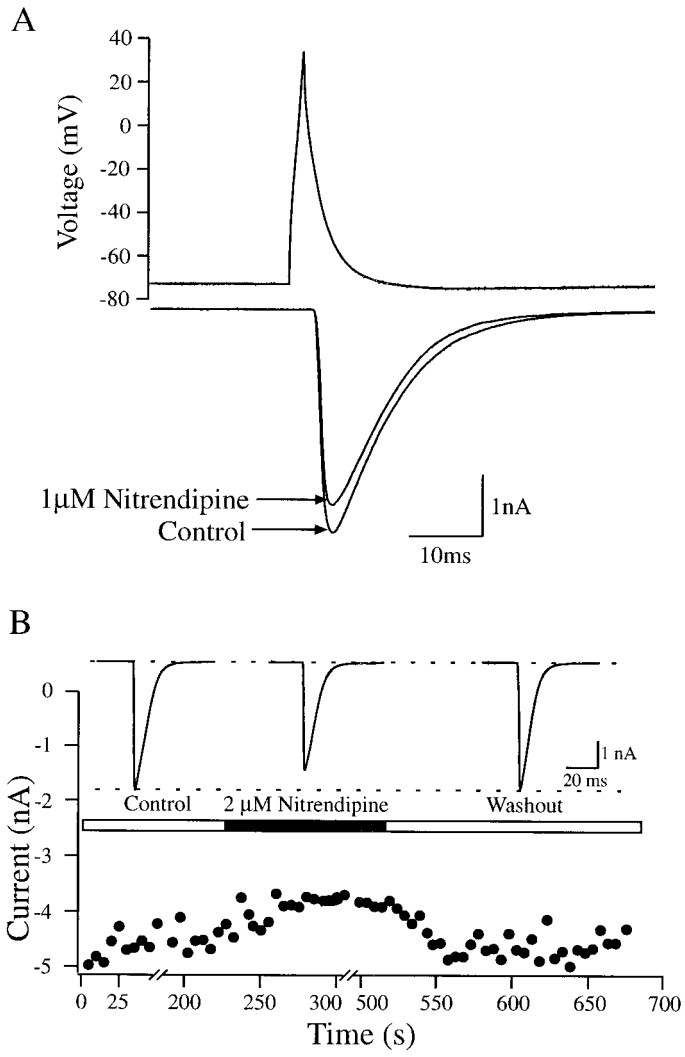

Figure 10. Nitrendipine inhibits evoked postsynaptic current. *A*, Simultaneous whole-cell recordings were made from a muscle and an overlying varicosity. Current injection into the varicosity initiated an action potential (*top trace*) that led to the generation of evoked synaptic currents. Average evoked synaptic current is shown before and after 1 μM nitrendipine (*bottom traces*). Each *trace* represents an average of 10 sweeps, and the average inhibition by nitrendipine in this cell was 12%. *B*, At a different synapse the postsynaptic current responses are triggered by a propagating action potential that was elicited by depolarization of the soma. The time course of peak EPC current before, during, and after application of 2 μM nitrendipine (*bottom*) is plotted along with three EPC *traces* (*top*). The *traces* each represent an average of 20 consecutive individual EPCs. The average inhibition by nitrendipine corresponded to 17% in this cell and is statistically significant (Student's t test, $p < 0.05$).

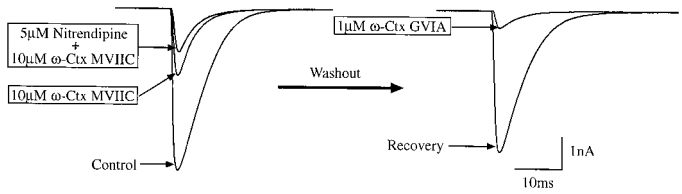

Figure 11. Synaptic current caused by L-type calcium channels is targeted by ω-Ctx GVIA but spared by ω-Ctx MVIIC. Simultaneous presynaptic and postsynaptic recordings were made as in Figure 10. *Left*, Synaptic current was inhibited by 57% after a 2 min exposure to 10 μM ω-Ctx MVIIC. Addition of 5 μM nitrendipine in the continued presence of ω-Ctx MVIIC reduced the synaptic current an additional 17%; 26% of the current remained unblocked. *Right*, A 10 min drug-free washout period recovered 90% of the synaptic current. Subsequent addition of 1 μM ω-Ctx GVIA reduced the current to 11% of the control value. Each *trace* represents an average of 10 sweeps. In the case of ω-Ctx GVIA, two failures were included in the average.

whether L-type current supports transmitter release (Yazejian et al., 1997). Emerging from all of these findings is the idea that N-type channels may be more effective than are other calcium channel types in mediating transmitter release.

Our findings indicate that distinct calcium channel isoforms, other than N-type channels, also contribute to ACh release at developing *Xenopus* neuromuscular junctions. However, arrival at this conclusion has required careful reevaluation of the specificity of pharmacological inhibitors of calcium current, most notably ω-Ctx GVIA. Since its original isolation (Olivera et al., 1984, 1985), a number of physiological studies have pointed to an action by ω-Ctx GVIA on N-type calcium channels. A specific and irreversible block of N-type channels by ω-Ctx GVIA was reported for fetal chick brain synaptosomes (Cruz and Olivera, 1986), mouse neuroblastoma-glioma cells (Kasai and Neher, 1992), rat pheochromocytoma cells and sympathetic neurons (Plummer et al., 1989), rat hippocampal neurons (Toselli and Taglietti, 1990), and rat dorsal root ganglion (DRG) neurons (Regan et al., 1991). However, some studies have brought into question the specificity of this toxin. ω-Ctx GVIA reversibly blocked L-type channels that were heterologously expressed in *Xenopus* oocytes (Williams et al., 1992) as well as native L-type channels in chick DRG neurons (Kasai et al., 1987; Aosaki and Kasai, 1989). In addition, irreversible block of both N- and L-type currents by ω-Ctx GVIA has been shown in chick DRG neurons (Fox et al., 1987; McCleskey et al., 1987), lizard presynaptic terminals (Lindgren and Moore, 1989), mouse motor neurons (Mynlieff and Beam, 1992), peptidergic terminals of the rat neurohypophysis (Wang et al., 1992), and rat sympathetic neurons (Hirning et al., 1988).

Our first hint that ω-Ctx GVIA blocked channel types other than N-type in *Xenopus* spinal neurons came from the observed supra-additivity of the average inhibition of calcium current by ω-Ctx GVIA and dihydropyridine antagonists. To exclude a nonspecific block of N-type channels by DHP, we showed that nitrendipine had no effect on the ω-Ctx MVIIC-sensitive calcium current in the soma of these spinal neurons. It is formally possible that the soma and varicosity express pharmacologically distinct N-type calcium channels and that only those in the varicosity are ω-Ctx GVIA sensitive. However, in view of previous reports showing inhibition of L-type channels by ω-Ctx GVIA and the following discussion, it is more likely that this toxin is not providing a specific block of N-type current in the varicosities.

Additional evidence of a nonspecific block by ω-Ctx GVIA was provided by experiments using ω-Ctx MVIIC, another toxin shown to block N-type channels. On average the equilibrium block of calcium current by ω-Ctx MVIIC was significantly lower than that by ω-Ctx GVIA, resulting in no supra-additivity of inhibition by ω-Ctx MVIIC and DHP antagonists. Furthermore, the sequential treatment by ω-Ctx MVIIC followed by ω-Ctx GVIA showed a significant difference in the ability of these two toxins to inhibit calcium current. As final evidence of the ability of ω-Ctx GVIA to block DHP-sensitive channels, the combined actions by ω-Ctx MVIIC and nitrendipine appeared to be no more effective than was ω-Ctx GVIA alone.

It is important to note that this L-type current also exhibits an

unusual pharmacology in that both DHP antagonists nitrendipine and nimodipine inhibit current at the appropriate concentrations, but the agonist Bay K8644 is without effect. This curious lack of effect of Bay K8644, as noted in previous studies (Hulsizer et al., 1991; Meriney et al., 1991), may point to the existence of a unique isoform in these terminals. Finally, it is important to indicate that at least one calcium channel isoform, in addition to those of L- and N-type, likely exists in varicosities. This type appears to be resistant to all drugs and toxins tested and, like the L-type channel, is not present in all terminals. Our overall averages place the contributions by N-type current at 60%, that by L-type current at 30%, and that by the drug-insensitive type at 9%.

A major advantage offered by the *Xenopus* coculture system is the ability to record simultaneously from both presynaptic and postsynaptic cells. Previous studies using this preparation have shown that N-type channels participate in release, but these studies failed to demonstrate involvement of additional calcium channel isoforms (Yazejian et al., 1997). In this study, we used the pharmacological profile of the individual channel types, established by presynaptic voltage-clamp measurements, to show that all three isoforms contribute to release. The nitrendipine-sensitive L-type contribution to evoked release averaged 13 ± 7% ($n = 5$), whereas the ω-Ctx MVIIC-sensitive N-type contribution averaged 60% ($n = 2$). This value for ω-Ctx MVIIC is likely an underestimate of the contribution of N-type channels to evoked release because of the subsaturating concentrations of ω-Ctx MVIIC used in these experiments. The toxin-resistant calcium current is credited with contributing 13% of the synaptic current. In the case of the L-type channel, the contribution to presynaptic calcium current (30%) appeared larger than the contribution determined on the basis of postsynaptic measurement (13%). Although it might be tempting to speculate that the L-type current couples less effectively to transmitter release than does the N-type channel, such quantitative comparisons cannot be made with the these data. Previous studies have shown that a highly nonlinear relationship exists between the amount of calcium entering presynaptic terminals and the quantity of transmitter released (Dodge and Rahamimoff, 1967).

How are our findings that multiple calcium channels contribute to release reconciled with previous studies that indicate N-type channels as the sole release channel? It is possible that L-type channels were not detected in previous studies because of their unusual pharmacological profile, as revealed via our current studies. Moreover, the physiological evidence supporting the idea that N-type channels account for all of the release is primarily based on the ability of ω-Ctx GVIA to block fully the evoked postsynaptic response at frog neuromuscular junctions (Kerr and Yoshikami, 1984; Koyano et al., 1987; Sano et al., 1987; Katz et al., 1995; Yazejian et al., 1997). Our finding that ω-Ctx GVIA, in addition to inhibiting N-type channels, also blocks L-type channels heightens the concern that previous studies may have failed to detect functional contributions by L-type channels in release. However, this argument does not explain the lack of effect of Bay K8644 and nimodipine on presynaptic calcium entry at adult neuromuscular junctions, nor does it account for labeling studies indicating the absence of L-type calcium channels in terminals of adult frogs (Robitaille et al., 1996).

An alternative means of reconciling our findings with the aforementioned studies is to conclude that developing nerve terminals differ from those of adult animals. Our studies were performed on embryonic nerve and muscle, and the presence of two calcium channel isoforms, in addition to the N-type, may be the consequence of an immature synapse. In support of this idea, studies have shown that a developmental switch occurs in some synapses in which the embryonic form expresses multiple types of calcium channels, whereas the adult form expresses a single type. For instance in developing terminals of chick ciliary ganglion neurons, transmitter release is sensitive to DHPs and ω-Ctx GVIA at stage 40 but is sensitive only to ω-Ctx GVIA after hatching (Gray et al., 1992). In the calyx of Held ω-Aga IVA completely suppresses EPCs by postnatal day 10. However, release at this central synapse is sensitive to both ω-Aga IVA and ω-Ctx GVIA during the period between postnatal days 4 and 7, and the ω-Ctx GVIA-sensitive component diminishes with development (Iwasaki and Takahashi, 1998). A similar developmental switch was seen at the rat neuromuscular junction. In 0- to 4-d-old rats both ω-Ctx GVIA and ω-Aga IVA reduced the amplitude of end-plate potentials (EPPs), whereas in 5- to 11-d-old rats EPPs could be reduced only by ω-Aga IVA (Rosato Siri and Uchitel, 1999). Finally, IPSCs recorded from deep cerebellar nuclear cells and thalamic relay cells could be inhibited by ω-Ctx GVIA and ω-Aga IVA early in development. ω-Ctx GVIA, however, had no effect after postnatal day 19, whereas ω-Aga IVA developed the ability to inhibit IPSCs completely by this stage (Iwasaki et al., 2000).

What advantages might be offered by the expression of two additional channel types during early synapse development? In our study, all of the calcium channel isoforms contribute to the EPC, repudiating the idea that only N-type channels can couple to release at this synapse. Instead, the presence of multiple calcium channel isoforms may serve to increase synaptic strength at a time in development when transmission is prone to failure. The contribution by multiple isoforms could increase the number of calcium channels thereby triggering a greater release of transmitter. This idea, however, assumes that the overall channel synthesis rate by a single gene is lower than the rate achieved in response to activation of multiple functionally redundant genes. Similar mechanisms may exist in the postsynaptic membrane of embryonic *Xenopus* skeletal muscle where multiple acetylcholine receptor types are expressed (Brehm et al., 1984b). Thus the expression of multiple isoforms of calcium channels and acetylcholine receptors may represent presynaptic and postsynaptic counterparts to the same overall strategy, that is, to ensure early onset of muscle contraction at critical stages of synaptogenesis.

REFERENCES

Anderson M, Kidokoro Y, Gruener R (1979) Correlation between acetylcholine receptor localization and spontaneous synaptic potentials in cultures of nerve and muscle. Brain Res 166:185–190.

Anderson MJ, Cohen MW, Zorychta E (1977) Effects of innervation on the distribution of acetylcholine receptors on cultured muscle cells. J Physiol (Lond) 268:731–756.

Aosaki T, Kasai H (1989) Characterization of two kinds of high-voltage-activated Ca channel currents in chick sensory neurons. Pflügers Arch 414:150–156.

Barry P, Lynch J (1991) Liquid junction potentials and small cell effects in patch-clamp analysis. J Membr Biol 121:101–117.

Borst J, Helmchen F, Sakmann B (1995) Pre- and postsynaptic whole-cell recordings in the medial nucleus of the trapezoid body of the rat. J Physiol (Lond) 489:825–840.

Brehm P, Kullberg R, Moody-Corbett F (1984a) Properties of non-junctional acetylcholine receptor channels on innervated muscle of *Xenopus laevis*. J Physiol (Lond) 350:631–648.

Brehm P, Kidokoro Y, Moody-Corbett F (1984b) Acetylcholine receptor channel properties during development of *Xenopus* muscle cells in culture. J Physiol (Lond) 357:203–217.

Buchanan J, Sun Y, Poo MM (1989) Studies of nerve–muscle interactions in *Xenopus* cell culture: fine structure of early functional contacts. J Neurosci 9:1540–1554.

Butz S, Okamoto M, Sudhof TC (1998) A tripartite protein complex with the potential to couple synaptic vesicle exocytosis to cell adhesion in brain. Cell 94:773–782.

Byerly L, Hagiwara S (1982) Calcium currents in internally perfused nerve cell bodies of *Limnaea stagnalis*. J Physiol (Lond) 322:503–528.

Cruz L, Olivera B (1986) Calcium channel antagonists. J Biol Chem 261:6230–6233.

Day N, Wood S, Ince P, Volsen S, Smith W, Slater C, Shaw P (1997) Differential localization of voltage-dependent calcium channel α_1 subunits at the human and rat neuromuscular junction. J Neurosci 17:6226–6235.

Del Castillo J, Katz B (1956) Localization of active spots within the neuromuscular junction of the frog. J Physiol (Lond) 132:630–649.

Dodge FA, Rahamimoff R (1967) Co-operative action of calcium ions in transmitter release at the neuromuscular junction. J Physiol (Lond) 193:419–432.

Dunlap K, Luebke J, Turner T (1995) Exocytotic Ca^{2+} channels in mammalian central neurons. Trends Neurosci 18:89–98.

Ellinor P, Zhang J, Randall A, Zhou M, Schwarz T, Tsien R, Horne W (1993) Functional expression of a rapidly inactivating neuronal calcium channel. Nature 363:455–458.

Fox A, Nowycky M, Tsien R (1987) Kinetic and pharmacological properties distinguishing three types of calcium currents in chick sensory neurones. J Physiol (Lond) 394:149–172.

Gray D, Bruses J, Pilar G (1992) Developmental switch in the pharmacology of Ca channels coupled to acetylcholine release. Neuron 8:715–724.

Hartsel S, Benz S, Ayenew W, Bolard J (1994) Na^+, K^+ and Cl^- selectivity of the permeability pathways induced through sterol-containing membrane vesicles by amphotericin B and other polyene antibiotics. Eur Biophys J 23:125–132.

Hillyard D, Monje V, Mintz I, Bean B, Nadasdi L, Ramachandran J, Miljanich G, Azimi-Zoonooz A, McIntosh J, Cruz L, Imperial J, Olivera B (1992) A new conus peptide ligand for mammalian presynaptic Ca^{2+} channels. Neuron 9:69–77.

Hirning L, Fox A, McCleskey E, Olivera B, Thayer S, Miller R, Tsien R (1988) Dominant role of N-type Ca channels in evoked release of norepinephrine from sympathetic neurons. Science 239:57–61.

Horn R, Marty A (1988) Muscarinic activation of ionic currents measured by a new whole-cell recording method. J Gen Physiol 92:145–159.

Hulsizer S, Meriney S, Grinnell A (1991) Calcium currents in presynaptic varicosities of embryonic motoneurons. Ann NY Acad Sci 635:424–428.

Iwasaki S, Takahashi T (1998) Developmental changes in calcium channel types mediating synaptic transmission in rat auditory brainstem. J Physiol (Lond) 509:419–423.

Iwasaki S, Momiyama A, Uchitel O, Takahashi T (2000) Developmental changes in calcium channel types mediating central synaptic transmission. J Neurosci 20:59–65.

Kasai H, Neher E (1992) Dihydropyridine-sensitive and ω-conotoxin-sensitive calcium channels in a mammalian neuroblastoma-glioma cell line. J Physiol (Lond) 448:161–188.

Kasai H, Aosaki T, Fukuda J (1987) Presynaptic Ca-antagonist ω-conotoxin irreversibly blocks N-type Ca-channels in chick sensory neurons. Neurosci Res 4:228–235.

Katz B, Miledi R (1967) The timing of calcium action during neuromuscular transmission. J Physiol (Lond) 189:535–544.

Katz E, Ferro P, Chersky B, Sugimori M, Llinas R, Uchitel D (1995) Effects of calcium channel blockers on transmitter release and presynaptic currents at the frog neuromuscular junction. J Physiol (Lond) 486:695–706.

Kerr L, Yoshikami D (1984) A venom peptide with a novel presynaptic blocking action. Nature 308:282–284.

Kidokoro Y, Brass B (1985) Redistribution of acetylcholine receptors during neuromuscular junction formation in *Xenopus* cultures. J Physiol (Lond) 80:212–220.

Kidokoro Y, Anderson M, Gruener R (1980) Changes in synaptic potential properties during acetylcholine receptor accumulation and neurospecific interactions in *Xenopus* nerve-muscle cell culture. Dev Biol 78:464–483.

Kostyuk P, Krishtal O (1977) Effects of calcium and calcium-chelating agents on the inward and outward current in the membrane of mollusc neurones. J Physiol (Lond) 270:569–580.

Koyano K, Abe T, Nishiuchi Y, Sakakibara S (1987) Effects of synthetic omega-conotoxin on synaptic transmission. Eur J Pharmacol 135:337–343.

Kullberg RW, Lentz TL, Cohen MW (1977) Development of the myotomal neuromuscular junction in *Xenopus laevis*: an electrophysiological and fine structural study. Dev Biol 60:101–129.

Leveque C, el Far O, Martin-Moutot N, Sato K, Kato R, Takahashi M, Seagar MJ (1994) Purification of the N-type calcium channel associated with syntaxin and synaptotagmin. A complex implicated in synaptic vesicle exocytosis. J Biol Chem 269:6306–6312.

Lindgren C, Moore J (1989) Identification of ionic currents at presynaptic nerve endings of the lizard. J Physiol (Lond) 414:201–222.

Llinas R, Steinberg IZ, Walton K (1981) Relationship between presynaptic calcium current and postsynaptic potential in squid giant synapse. Biophys J 33:323–352.

Llinas R, Sugimori M, Lin J, Cherksey B (1989) Blocking and isolation of a calcium channel from neurons in mammals and cephalopods utilizing a toxin fraction (FTX) from funnel-web spider poison. Proc Natl Acad Sci USA 86:1689–1693.

Luebke J, Dunlap K, Turner T (1993) Multiple calcium channel types control glutamatergic synaptic transmission in the hippocampus. Neuron 11:895–902.

McCleskey EW, Fox AP, Feldman DH, Cruz LJ, Olivera BM, Tsien RW, Yoshikami D (1987) ω-Conotoxin: direct and persistent blockade of specific types of calcium channels in neurons but not muscle. Proc Natl Acad Sci USA 84:4327–4331.

McDonough SI, Swartz KJ, Mintz IM, Boland LM, Bean BP (1996) Inhibition of calcium channels in rat central and peripheral neurons by ω-conotoxin MVIIC. J Neurosci 16:2612–2623.

Meriney S, Hulsizer S, Grinnell A (1991) Calcium currents in varicosities of motoneuron neurites ending on muscle cells *in vitro*. Biomed Res 12:53–55.

Mynlieff M, Beam K (1992) Characterization of voltage-dependent calcium currents in mouse motoneurons. J Neurophysiol 68:85–92.

Neher E (1992) Correction for liquid junction potentials in patch clamp experiments. Methods Enzymol 207:123–131.

Nieuwkoop PD, Faber J (1956) Normal table of *Xenopus laevis* (Daudin). Amsterdam: North-Holland.

Nowycky M, Fox A, Tsien R (1985) Three types of neuronal calcium channel with different calcium agonist sensitivity. Nature 316:440–443.

Olivera B, McIntosh J, Cruz L, Luque F, Gray W (1984) Purification and sequence of a presynaptic peptide toxin from *Conus geographus* venom. Biochemistry 23:5087–5090.

Olivera B, Gray W, Zeikus R (1985) Peptide neurotoxins from fish hunting cone snails. Science 230:1338–1343.

Peng H, Nakajima Y, Bridgman P (1980) Development of the postsynaptic membrane in *Xenopus* neuromuscular cultures observed by freeze-fracture and thin-section electron microscopy. Brain Res 196:11–31.

Plummer M, Logothetis D, Hess P (1989) Elementary properties and pharmacological sensitivities of calcium channels in mammalian peripheral neurons. Neuron 2:1453–1463.

Protti D, Reisin R, Mackinley TA, Uchitel OD (1996) Calcium channel blockers and transmitter release at the normal human neuromuscular junction. Neurology 46:1391–1396.

Randall A, Tsien R (1995) Pharmacological dissection of multiple types of Ca^{2+} channel currents in rat cerebellar granule neurons. J Neurosci 15:2995–3012.

Regan L, Sah D, Bean B (1991) Ca^{2+} channels in rat central and peripheral neurons: high threshold current resistant to dihydropyridine blockers and ω-conotoxin. Neuron 6:269–280.

Regehr WG, Mintz IM (1994) Participation of multiple calcium channel types in transmission at single climbing fiber to Purkinje cell synapses. Neuron 12:605–613.

Robitaille R, Adler E, Charlton M (1990) Strategic location of calcium channels at transmitter release sites of frog neuromuscular synapses. Neuron 5:773–779.

Robitaille R, Bourque MJ, Vandaele S (1996) Localization of L-type Ca^{2+} channels at perisynaptic glial cells of the frog neuromuscular junction. J Neurosci 16:148–158.

Rosato Siri M, Uchitel O (1999) Calcium channels coupled to neurotransmitter release at neonatal rat neuromuscular junctions. J Physiol (Lond) 514:533–540.

Sano K, Enomoto K, Maeno T (1987) Effects of synthetic ω-conotoxin, a new type Ca^{2+} antagonist, on frog and mouse neuromuscular transmission. Eur J Pharmacol 141:235–241.

Sheng Z, Rettig J, Takahashi M, Catterall WA (1994) Identification of a syntaxin-binding site on N-type calcium channels. Neuron 13:1303–1313.

Stanley E, Goping G (1991) Characterization of a calcium current in a vertebrate cholinergic presynaptic nerve terminal. J Neurosci 11:985–993.

Takahashi T, Nakajima Y, Hirosawa K, Nakajima S, Onodera K (1987) Structure and physiology of developing neuromuscular synapses in culture. J Neurosci 7:473–481.

Tarelli FT, Passafaro M, Clementi F, Sher E (1991) Presynaptic localization of ω-conotoxin-sensitive calcium channels at the frog neuromuscular junction. Brain Res 547:331–334.

Toselli M, Taglietti V (1990) Pharmacological characterization of voltage-dependent calcium currents in rat hippocampal neurons. Neurosci Lett 112:70–75.

Turner T, Adams M, Dunlap K (1993) Multiple Ca^{2+} channel types coexist to regulate synaptosomal neurotransmitter release. Proc Natl Acad Sci USA 90:9518–9522.

Wang X, Treistman S, Lemos J (1992) Two types of high threshold calcium currents inhibited by omega-conotoxin in nerve terminals of rat neurohypophysis. J Physiol (Lond) 445:181–199.

Westenbroek RE, Hoskins L, Catterall WA (1998) Localization of Ca^{2+} channel subtypes on rat spinal motor neurons, interneurons, and nerve terminals. J Neurosci 18:6319–6330.

Williams M, Feldman D, McCue A, Brenner R, Velicelebi G, Ellis S, Harpold M (1992) Structure and functional expression of α_1, α_2 and β subunits of a novel human neuronal calcium channel subtype. Neuron 8:71–84.

Yawo H, Momiyama A (1993) Re-evaluation of calcium currents in pre- and postsynaptic neurones of the chick ciliary ganglion. J Physiol (Lond) 460:153–172.

Yazejian B, DiGregorio D, Vergara J, Poage R, Meriney S, Grinnell A (1997) Direct measurements of presynaptic calcium and calcium-activated potassium currents regulating neurotransmitter release at cultured *Xenopus* nerve–muscle synapses. J Neurosci 17:2990–3001.